How Physical Carrier Sense Affects Protocol Capacity in Multi-hop Wireless Networks: Modeling and Analysis

Zheng Zeng, Yong Yang and Jennifer C. Hou
Dept. of Computer Science
University of Illinois at Urbana-Champaign
Urbana, IL 61801
{zzeng2, yang25, jhou}@uiuc.edu

ABSTRACT

In recent years, wireless ad hoc networks have become increasingly popular in both military and civilian applications due to its capability of building networks without the need for a pre-existing infrastructure. While a number of studies have been carried out to study the performance of IEEE 802.11 DCF in single-cell wireless LANs, the analysis of IEEE 802.11 DCF in multi-hop wireless networks with consideration of the effects of physical carrier sense, SINR, and collision caused by accumulative interference has been lacking. In this paper, we substantially extend Calí's work and rigorously model, with these effects considered, channel activities governed by IEEE 802.11 DCF in multi-hop wireless networks. We show that as in single-cell WLANs, the choice of the contention window size can greatly impact the system throughput in multi-hop wireless networks. However, the optimal value of the contention window size is quite different. Moreover, the optimal attempt probability p (the optimal window size) derived for multi-hop wireless networks with respect to maximizing the systems throughput is larger (smaller) than that for single-cell WLANs. We also show that, given the minimal SINR threshold β, the optimal carrier sense range is smaller than the conventional value used (provided that the contention window size is tuned accordingly).

1. INTRODUCTION

Because the medium in wireless networks is by nature shared among nodes in the spatial domain, media access control (MAC) plays an important role of coordinating medium access among nodes. The IEEE 802.11 [1] distributed coordination function (DCF) protocol is a CSMA/CA MAC protocol that has been widely studied and used in wireless networks because of its distributed nature and ease of implementation. Essentially DCF arbitrates medium access with two mechanisms: *carrier sense multiple access* for detecting simultaneous transmissions and for mitigating interference and *binary exponential back-off mechanism* for resolving contention.

DCF carrier sense can be categorized into *virtual* carrier sense and *physical* carrier sense. In this paper we focus on the latter. Before attempting for transmission, a node senses the medium and defers its transmission if the channel is sensed busy, i.e., the strength of the received signal exceeds a certain threshold CS_{th}. Carrier sense reduces the likelihood of collision by preventing nodes in the vicinity of each other from transmitting simultaneously, while allowing nodes that are separated by a safe margin (termed as the carrier sense range, R_{cs}) to engage in concurrent transmissions. The latter effect is referred to as *spatial reuse*. In multi-hop wireless networks, the choice of the carrier sense range depends on CS_{th} and the minimum Signal-to-Interference-and-Noise-Ratio (that gives the minimal SINR at which the received signal can be correctly decoded). If the transmit power of all the nodes is the same, a large value of CS_{th} implies a small value of R_{cs} (i.e., better degree of spatial reuse), but the interference to be tolerated by the transmission may be also high. A small value of CS_{th}, on the other hand, implies a larger value of R_{cs}, but the resulting SINR will be comparatively higher.

Several research efforts have been made to understand the impact of carrier sense and spatial reuse on system performance. Zhu *et al.* [8] attempt to identify the optimal carrier sense threshold that maximizes spatial reuse in a regular topology. Jamieson *et al.* [7] carry out an empirical study to understand the limitation of carrier sense. Yang and Vaidya [13] show that the MAC layer overhead has a great impact on the choice of the carrier sensing range and the data rate. Zhai and Feng [14] point out that the carrier sense threshold that maximizes the network capacity does not vary significantly with the channel data rates.

The binary exponential back-off mechanism, on the other hand, aims to resolve collision. If nodes that are spatially close to each other sense the medium to be idle and transmit simultaneously, collisions occur. Alternatively, the accumulative interference contributed by the concurrent transmissions of multiple nodes outside the carrier sense range could be so significant that it corrupts the transmission. The binary exponential back-off mechanism is designed to deal with these situations. Each node must wait for a time interval specified by the contention window, before it starts to transmit (after sensing the channel idle for DIFS). An adequate contention window size reduces the collision probability, while not wasting the bandwidth by having all the nodes busy backing off.

There have been several models that characterize the transmission activities governed by IEEE 802.11 DCF and study how to tune the contention window size in single-cell WLANs. (See, for example, [9] for an excellent survey.) Calí *et al.* [4] and Bianchi [2] devise, respectively, two analytical models to calculate the system capacity in WLANs. In particular, Bianchi [2] models the behavior of the binary backoff counter at one tagged station as a discrete Markov chain model. Calí *et al.* [4] derive a theoretical throughput bound by approximating IEEE 802.11 with a p-persistent model of IEEE 802.11. Both observe that the system throughput only relies on the contention window size and the number of active stations. They also show that with the current parameter settings of IEEE 802.11, the maximal achievable system throughput falls far beneath the theoretical capacity bound. Kumar *et al.* [10] present a fixed point analysis of Bianchi's model in the asymptotic regime of a large number of stations, and give explicit expressions for the collision probability, the aggregate attempt rate, and the aggregate throughput. All these studies focus on single-cell wireless LANs.

Medepalli and Tobagi [12] extend Bianchi's model to accommodate the effect of hidden/exposed nodes in *multi-hop* wireless networks. They show that the minimum contention window size used in the exponential back-off mechanism has a more profound effect on mitigating flow starvation than the maximum contention window size. What has not been exclusively addressed in the study is (i) the impact of carrier sense threshold (that determine the sharing range of the wireless medium and hence the extent of spatial reuse) on the system performance and (ii) the interplay between the carrier sense threshold and the contention window size.

In this paper, we propose an analytical model that extends Calí's model to multi-hop wireless networks and incorporates the effects of physical carrier sense, SINR, and collision caused by accumulative interference. The major difficulty in modeling multi-hop wireless networks lies in that the carrier sense threshold CS_{th} plays an important role in several aspects. First, when node i attempts for transmission, it has to ensure that the received signal strength does not exceed CS_{th}. In WLANs, this means all the other nodes do not transmit at the time of physical carrier sense. However, in multi-hop wireless networks, this merely means that all the nodes within the carrier sense range R_{cs} of node i do not transmit.[1] Second, the condition for successful transmission in WLANs is that no more than one nodes attempt to transmit *simultaneously*. Once the transmission of a node starts, all the other nodes will sense a busy medium and be silenced. However, in multi-hop wireless networks, after a node senses an idle medium and starts transmission, nodes outside R_{cs} may still engage in new transmissions, adding to the level of interference. Whether or not node i's transmission succeeds then depends on the *Signal-to-Interference-and-Noise-Ratio* (SINR) — if the SINR perceived by node i is smaller than a minimum SINR threshold β, the transmission cannot be correctly decoded and is thus failed. CS_{th} is a tunable parameter that controls spatial reuse and transmission quality (as determined by interference among concurrent transmissions). A larger value of CS_{th} allows better spatial reuse at the expense of increased interference (and hence the likelihood of frames being corrupted because of accumulative interference). The impact of CS_{th} on the systems throughput has not been extensively studied (at the level as detailed as that in Calí's model).

In our proposed model, we follow Calí's methodology of characterizing the time interval of two consecutive successful transmissions as the *virtual transmission time*, t_v, and derive its expected value. We faithfully incorporate all the aforementioned effects that CS_{th} makes in multi-hop wireless networks, and derive $E(t_v)$ *as perceived by nodes in one interference range.* (The reason for choosing the "cell" as nodes within an interference range will be elaborated on in Section 3.) We validate the derived model via simulation, and make several important implications from the analytical model.

The rest of this paper is organized as follows. In Section 2 we summarize Calí's model and the Hexagon interference model [11] that will be used throughout the paper. In Section 3, we present the analytical model that characterizes the transmission activities governed by IEEE 802.11 DCF in multi-hop wireless networks. In Section 4, we

[1]Note that we do not consider channel errors in this paper.

Table 1: Systems parameters used throughout the paper.

Parameter	Description
M	Number of active hosts
p	Probability that each node attempts for transmission when the medium is sensed idle
q	Parameter for the geometric distribution of the packet size, i.e., $\Pr\{\text{packet\_length} = \text{i slot}\} = q^{i-1}(1-q)$.
$\bar{m}$	Average transmission time, i.e., $\bar{m} = t_{slot}/(1-q)$
τ	Maximum propagation time
DIFS	Distributed interframe spacing
SIFS	Short interframe spacing
EIFS	Extended interframe spacing
ACK	Time required to transmit the ACK
N_c	Number of collisions in a virtual transmission time
$E(T_c)$	Average length of a collision period
$E(I)$	Average duration of consecutive idle slots before a successful transmission or a collision
$E[S]$	Time required to complete a successful transmission (including all the protocol overheads), i.e., $E(S) = \bar{m} + SIFS + ACK + DIFS$.

discuss several hints we can get from the derived model. In Section 5, we validate the proposed model via simulation and make several important observations from both the analytical/simulation results. Finally, we conclude the paper in Section 6 with a list of future research agendas.

2. BACKGROUND MATERIAL

In this section, we summarize 1) the p-persistent model of IEEE 802.11 DCF proposed by Calí *et al.* [4][5]; 2) the hexagon interference model which describes the worst-case interference which a wireless (receiver) node may experience with the use of physical carrier sense. These models will be leveraged throughout the paper.

2.1 p-persistent Model That Characterizes IEEE 802.11 DCF in WLANs

For analytical tractability, Calí *et al.* [5, 4] consider a *p-persistent* version of IEEE 802.11 DCF, which differs from the standard protocol only in the selection of the backoff interval. Instead of using the binary exponential backoff timer values, the *p-persistent* version determines its backoff interval by sampling from a geometric distribution with parameter p. Due to the memoryless property of this geometric-distributed backoff algorithm, it is more tractable to analyze the *p-persistent* IEEE 802.11 protocol.

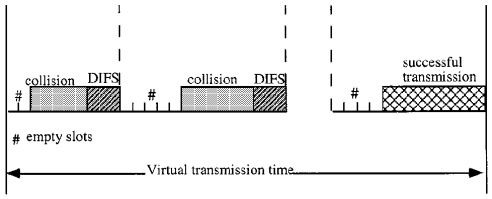

Figure 1: Structure of virtual transmission time.

The analytic model is derived under the assumption that all the stations always have packets ready for transmission (which is termed the *asymptotic* condition in [5, 4]). Under the geometrically-distributed backoff assumption, the process that characterizes the occupancy behavior of the channel (idle slots, collisions, and successful transmission) till the end of each successful transmission is regenerative, with the sequence of time instants corresponding to the completion of successful transmission being the regenerative points. Calí *et al.* exploit this regenerative property and define the jth virtual transmission time as the time interval between the jth and *(j+1)*th successful transmissions. As shown in Figure 1, idle periods and collisions precede a successful transmission, where an idle period is a time interval in which the channel is idle due to the fact that all the back-logged stations are in the back-off mode, and a collision is the interval in which two or more stations attempt for transmission and their packets collide with one another.

Let t_v be defined as the average virtual transmission time, I_i and $T_{c,i}$ as the length of the ith idle period and the length of the ith collision in a virtual transmission time respectively. Given the major system parameters in Table 1, the protocol capacity ρ can be expressed as

$$\rho = \frac{\bar{m}}{t_v}, \tag{1}$$

where

$$\begin{aligned} t_v &= E\left(\sum_{i=1}^{N_c}(DIFS + I_i + T_{c,i} + SIFS)\right) + \\ &\quad (N_c+1)\cdot E(I) + E(S) \\ &= E(N_c)\cdot(E(T_c) + DIFS + SIFS) + (E(N_c)+1)\cdot \\ &\quad E(I) + \bar{m} + SIFS + ACK + DIFS. \end{aligned} \tag{2}$$

Note that $SIFS$ and ACK in the first term on the right hand side of Eq.(2) is due to the extra waiting period in EIFS after detection of an incorrectly-received frame (i.e., frame collision). Note that in Calí's model, it is assumed that each station waits for an interval of DIFS after a frame collision, while we assume the use of EIFS here.

The expressions of $E(N_c)$, $E(T_c)$, and $E(I)$ have

been derived for WLANs [5, 4]:

$$E(N_c) = \frac{1-(1-p)^M}{Mp(1-p)^{M-1}} - 1, \quad (3)$$

$$E(T_c) = \frac{t_{slot}}{1-(1-p)^M - Mp(1-p)^{M-1}} \times [\sum_{h=0}^{\infty}\{h \times [(1-pq^h)^M - (1-pq^{h-1})^M]\} - \frac{Mp(1-p)^{M-1}}{1-q}], \quad (4)$$

$$E(I) = \frac{(1-p)^M}{1-(1-p)^M} \times t_{slot}. \quad (5)$$

2.2 Hexagon Interference model

The hexagon interference model has been used to to calculate the worst-case SINR given that every node senses the medium before attempting for transmission. Specifically, let P denote the transmission power used by a sender, P_r the received power at the corresponding receiver, r is the distance between the sender and the receiver, and θ is the path loss exponent (which usually ranges from 2 (free space) to 4 (two-ray ground)). Then we have

$$P_r = \frac{P}{r^\theta}. \quad (6)$$

With this radio propagation model, we can derive the relation between the *carrier sense range*, R_{cs}, and the carrier sense threshold, CS_{th}:

$$CS_{th} = \frac{P}{R_{cs}{}^\theta}. \quad (7)$$

In order to decode the received signal correctly, the received signal is required to exceed a threshold called the *receive sensitivity* (RX_{th}). By Eq. (6), the maximum transmission range R_{tx} can be calculated as

$$R_{tx} = (\frac{P}{RX_{th}})^{\frac{1}{\theta}}. \quad (8)$$

Let X be defined as the ratio between R_{cs} and the transmission range R_{tx}, i.e., $X \triangleq \frac{R_{cs}}{R_{tx}}$.

Figure 2 shows the scenario in which the receiver D_0 incurs the worst-case interference. Note that D_i is the intended receiver of sender N_i ($1 \le i \le 6$), and the distance between N_i and D_i is R_{tx}. By the definition of CS_{th}, the distance between any two adjacent senders is at least R_{cs}. N_1–N_6 constitute the six 1^{st} tier interference nodes that are located at the closest possible locations to D_0. Let P_r denote the power received at D_0 from N_0 and $P_{r,i}$ the power received at D_0 from N_i. It has been shown in [11] that the worst case interference (and hence the smallest SINR at receiver D_0) is incurred when D_0 is so positioned that the six 1^{st} tier interference nodes are, respectively, of distance $R_{cs} - R_{tx}$, $R_{cs} - R_{tx}$, $R_{cs} - R_{tx}/2$, R_{cs}, $R_{cs} + R_{tx}/2$, and $R_{cs} + R_{tx}$ away from it, as illustrated in Figure 2. The corresponding worst-case $SINR$ at receiver D_0 is expressed expressed in Eq. (9).[2]

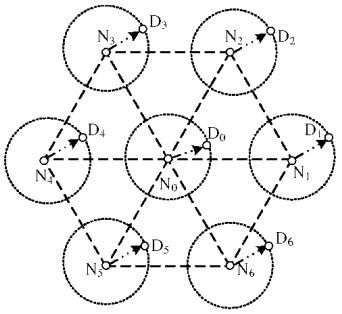

Figure 2: Interference Model. D_i is the intended receiver of sender N_i ($1 \le i \le 6$).

Note that the hexagon model errs on the pessimistic side for the following reasons. First, the worst-case interference only occurs when there are six nodes located exactly at the desired locations, which rarely happens in a random topology. Second, use of physical carrier sense usually prevents such an extreme case from taking place. As shown in Figure 2, if N_0 starts transmission first, then N_i may initiate a concurrent transmission because it is outside the carrier sense range of N_0. Now the accumulative (interference) signal strength at N_{i-1} (or N_{i+1}) is $2\times\mathrm{CS}_{th}$, which prevents N_2 from initiating a concurrent transmission until N_0 or N_i completes its transmission. In general, although the number of 1^{st} tier interference nodes is six, not all of them can locates at the worst case location.

Given that the hexagon model errs on the pessimistic side and is too conservative, one may consider only the interference from one closest interference node which is R_{cs}-R_{tx} away from receiver D_0. In this case, the SINR at receiver D_0 is

$$SINR = (X-1)^\theta. \quad (10)$$

Given the minimal SINR threshold β and the transmit power P (which in turn determines R_{tx} by Eq. (8)), one can determine the value of CS_{th} by the following steps: (1) obtaining the value of X using either Eq. (9) $= \beta$ or Eq. (10) $= \beta$; (2) obtaining the value of R_{cs} by $X = \frac{R_{cs}}{R_{tx}}$, and the value of CS_{th} by Eq. (7). Let $CS_{th,1}$ and $CS_{th,2}$ denote the CS_{th} derived using Eq. (9) and (10), respectively. We have $CS_{th,1} < CS_{th,2}$. However, the optimal value of CS_{th} is even larger than $CS_{th,2}$. This will be corroborated in our simulation study in Section 5. Moreover, both our proposed analytical model and simulation results indicate that, when CS_{th} is slightly smaller than

[2]Note that we ignore the background noise in the expression.

$$SINR = \frac{\frac{P}{R_{tx}^{\theta}}}{\frac{2P}{(R_{cs}-R_{tx})^{\theta}} + \frac{P}{(R_{cs}-R_{tx}/2)^{\theta}} + \frac{P}{R_{cs}^{\theta}} + \frac{P}{(R_{cs}+R_{tx}/2)^{\theta}} + \frac{P}{(R_{cs}+R_{tx})^{\theta}}} = \frac{1}{\frac{2}{(X-1)^{\theta}} + \frac{1}{(X-1/2)^{\theta}} + \frac{1}{(X)^{\theta}} + \frac{1}{(X+1/2)^{\theta}} + \frac{1}{(X+1)^{\theta}}} \quad (9)$$

$CS_{th,2}$, although it cannot completely prevent collision caused by multiple concurrent transmissions from taking place, it can still keep the collision probability low, while achieving better spatial reuse.

3. ANALYTICAL MODEL

In this section, we present our analytical model that extends Calí's work to multi-hop wireless networks, with consideration of the effects of physical carrier sense, SINR, and collision caused by accumulative interference (as a result of concurrent transmissions). Recall that Calí *et al.* use their model to derive the optimal value of the attempt probability p (and hence the contention window size) that maximizes the protocol capacity. Similarly, the systems throughput derived in our model will be a function of p, the carrier sense threshold CS_{th}, the minimum SINR threshold β, and the node density, λ, in the network. Given the minimum SINR threshold β and the node density λ (which are considered part of the network configuration), we can (numerically) obtain the optimal combination of (p, CS_{th}) that maximizes the systems throughput in a multi-hop wireless network.

3.1 Assumptions and Notations

The following assumptions have been made to devise the analytical model:

(A1) Nodes are distributed on a plane according to a Poisson point process with node density λ.

(A2) Every node uses the same power P. The maximum transmission range R_{tx} can then be determined from Eq. (8) given the receive sensitivity RX_{th}.

(A3) The radio propagation model is given in Eq. (6). For a transmission to be successful, the SINR at the receiver must exceed the minimum SINR threshold β.

(A4) If the carrier sense threshold CS_{th} is determined, the corresponding *carrier sense radius* R_{cs} is determined by Eq. (7).

(A5) Whether a node decides to access the media is independent of others. This is referred to as the independent access assumption.

(A6) To derive the accumulative interference contributed by nodes that are outside R_{cs} of an intended receiver, we only consider the six 1^{st}-tier interference nodes (e.g., N_1-N_6 in Fig. 2). As indicated in [6][3], the interference contributed by these six interference nodes dominate.

Note that while **(A1)**-**(A4)** are consistent with PHY/MAC operations in realistic settings, **(A5)**-**(A6)** are approximations.

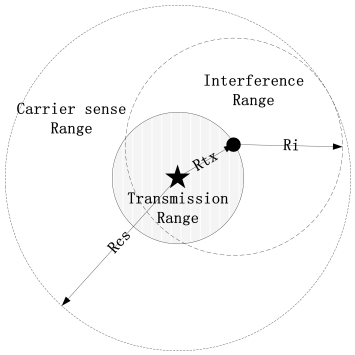

Figure 3: Definition of transmission range, interference range, and carrier sense range.

The major system parameters are given in Table 1. To ensure that any on-going transmission will not be corrupted by its closest possible competing sender, we should have that Eq. (10) $\geq \beta$. This implies

$$X = \frac{R_{cs}}{R_{tx}} \geq \beta^{\frac{1}{\theta}} + 1. \quad (11)$$

Eq. (11) gives a lower bound on the value of "safe" R_{cs}. Also, given an on-going transmission, we define the interference range as a circle centered at the receiver with radius R_i. If any node within the interference range transmits, the on-going transmission is corrupted at the receiver. Specifically,

$$\frac{P/R_{tx}^{\theta}}{P/R_i^{\theta}} \leq \beta \Longrightarrow R_i \leq \beta^{\frac{1}{\theta}} \times R_{tx}. \quad (12)$$

Figure 3 depicts the transmission range, interference range, and carrier sense range with respect to one transmission.

3.2 Model Overview

We follow Calí's methodology of characterizing and deriving the *virtual transmission time*. However, we have to consider the following aspects in multi-hop wireless networks:

1. We *re-define* the number of active nodes (M). In a WLAN, M is the number of active nodes in the WLAN. However, in a multi-hop wireless network the notion of a "cell" (in which the system view is applied) has to be defined. In this paper, we define the "cell" A to be a circle with the interference range, R_i^2, as the radius, i.e., $A = \pi R_i^2$, and M be all the nodes located in A. We will elaborate on the rationale in Section 3.3.

2. We consider other possibilities that may lead

to an idle period before either a successful transmission or a collision (Figure 1). In a WLAN, an idle period is consecutive idle slots in which all the back-logged nodes are in the back-off mode. However, in a multi-hop network, an idle period may also occur in A when all the nodes in A are being silenced by senders outside A but within the carrier sense ranges of these nodes. We will discuss how we take into account of various possibilities in calculating $E[I]$ in Section 3.4.

3. We re-derive the attempt probability p. Specifically, let E denote the event that the "cell" is idle and E_1 the event that a node *senses* the medium to be idle. Also, let $p \stackrel{\triangle}{=} \Pr(\text{a node attempts for transmission } |E)$ and $p_1 \stackrel{\triangle}{=} \Pr(\text{a node attempts for transmission } |E_1)$. It has been shown in [4] that $p_1 = 2/(E(CW)+1)$ in a WLAN. Moreover, because $E \equiv E_1$ in a WLAN, we have $p = p_1$. However, in a multi-hop wireless network, with the accumulative interference outside the interference range taken into account, $E_1 \subset E$, and p_1 alone is not sufficient to characterize the access probability. We will discuss how we re-derive p in Section 3.5.

4. We enumerate and consider all possible causes of collisions in multi-hop wireless networks. In a WLAN, collisions are only caused by simultaneous transmissions within the WLAN. However, in a multi-hop wireless network, collisions also occur when the accumulative interference contributed by *simultaneous* transmissions outside the interference range and/or *concurrent* transmissions outside the carrier sense range. We will discuss how we take into account of all these factors into calculating the collision probability P_c and the collision period N_c in Section 3.6.

3.3 Definition of a Cell in Multi-hop Wireless Networks

Recall that Calí's model characterizes transmission activities governed by DCF in a WLAN with M active nodes *from the system view*. To adapt Calí's model to a multi-hop wireless network, the first step is to define the notion of a "cell." As such, we divide the plane into "cells" of area $A = \pi R_i^2$, and focus on the system view of a "cell." The rationale for using the interference range R_i as the radius of a "cell" is as follows. In a WLAN, an on-going transmission is successful if and only if no other transmissions overlap in time with the on-going transmission. To extend Calí's model to multi-hop wireless networks, the same property should hold. By the definition of the interference range R_i (Eq. (12)), we know that at most one transmission is allowed in the interference range of a receiver at any time in order for the transmission to be successful. If any node within the interference range of an intended receiver transmits, it corrupts the corresponding transmission. Therefore we choose the "cell" A to be of area πR_i^2 and set M to be the number of active nodes within an interference range, i.e., $M = \lambda \pi {R_i}^2$.

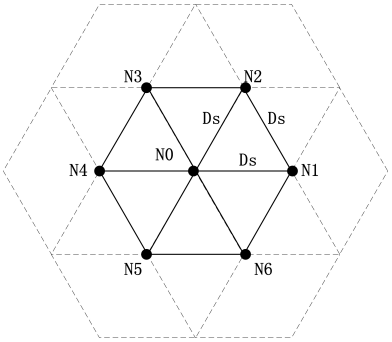

Figure 4: Definition of the silence range

With the new definition of a "cell," $packet\_size/t_v$ characterizes the system throughput within one "cell" A whose area depends on the minimum SINR threshold β (as R_i depends on β (Eq. (12))). Note that β determines the data rate at which a sender can sustain — the larger the β value, the larger the achievable data rate.

3.4 Derivation of the Idle Period

Recall that in a multi-hop network, an idle period may occur in A when all the nodes in A are being silenced by senders outside A but within the carrier sense ranges of these nodes. That is, the idle period may also be the time interval during which the "cell" is silenced by the transmissions in other "cells".

In order to incorporate this effect, we define the *silence area* A_S to be the area that is silenced by a transmission. Consider Figure 4 which depicts the best spatial reuse that can be achieved when N_0 and N_1-N_6 can simultaneously engage in successful transmissions. Let D_s denote the distance between any two concurrent transmissions. Then N_0–N_6 are located at a distance of D_s away from from N_0, which yields the best spatial reuse. (Note that D_s is not equal to R_{cs}, because as explained in Section 2.2, not all the first-tier interference nodes located at a distance of R_{cs} can transmit at the same time.) Without loss of generality, consider the interference N_0 experiences. In order for N_0 to succeed in its transmission, the aggregate interference contributed by N_1–N_6 should be less than or equal to CS_{th}, i.e.,

$$6 \cdot \frac{P}{D_s^\theta} \le CS_{th} = \frac{P}{R_{cs}^\theta} \Longrightarrow D_s \ge R_{cs} \times 6^{\frac{1}{\theta}}. \quad (13)$$

The spatial reuse is maximized when the equality holds. In this case, every sender occupies an area

that is composed of six small triangles, while each triangle is shared by three senders. As a result, the *silence area* of a transmission is the area of two triangles.

$$A_S = \frac{\sqrt{3}}{2} \times {D_s}^2 = \frac{\sqrt{3}}{2} \times (R_{cs} \times 6^{\frac{1}{\theta}})^2. \quad (14)$$

Let $M_s \triangleq \lambda A_S$ denote the number of nodes in a silence area and φ the ratio of M_s to M ($\varphi \triangleq M_s/M$). When a node transmits, it silences not only nodes within its interference range, but also nodes within its silence area. As a matter of fact, the transmission inside an interference range may silence nodes in its $\varphi - 1$ neighboring interference ranges.

Now let $E[I_1]$ and $E[I_2]$ denote, respectively, the average number of times the medium is idle due to the event that all the nodes inside the "cell" are in the back-off mode and the event that all the nodes are silenced by transmissions outside the interference range. If an idle period is caused by transmission(s) in other interference ranges, it lasts for for the duration of a frame transmission, i.e. $\bar{m} = (\mathrm{t}_{slot}/\text{1-q})$. The idle period is thus redefined as

$$E[I]{=}E[I_1] \times \frac{t_{slot}}{1-q} + E[I_2] \times t_{slot}. \quad (15)$$

No matter which event causes an idle period, the probability that an idle period occurs is $(1-p)^M$ and the number of times idle periods occur follows a geometric distribution with $(1-p)^M$. Consequently,

$$E[I_1] + E[I_2] = \frac{(1-p)^M}{1-(1-p)^M}. \quad (16)$$

With probability $(1-(1-p)^{M(\varphi-1)})$, at least one sender in the other $(\varphi-1)$ interference ranges is transmitting, and hence the average number of times idle periods occur because of the second event is

$$E[I_2] = \frac{(1-p)^M}{1-(1-p)^M} \times [1-(1-p)^{M(\varphi-1)}]. \quad (17)$$

Finally $E[I]$ can be expressed as

$$E[I]{=}\frac{(1-p)^M \times t_{slot}}{1-(1-p)^M} \times \left[\frac{1-(1-p)^{M(\varphi-1)}}{1-q} + (1-p)^{M(\varphi-1)}\right] \quad (18)$$

3.5 Derivation of Attempt Probability p

Let E denote the event that the "cell" is idle, and $p \triangleq \Pr(\text{a node attempts for transmission } |E)$. Also, let E_1 denote the event that a node *senses* the medium to be idle, and $p_1 \triangleq \Pr(\text{a node attempts for transmission } |E_1)$. It has been shown in [4] that $p_1 = 2/(E(CW)+1)$ in a WLAN. This, coupled with the fact that $E \equiv E_1$ (because every node hears every one else), leads to $p = p_1 = 2/(E(CW)+1)$. However, $E_1 \subset E$ in a multi-hop wireless network due to the accumulative interference outside the interference range. As a result, $p \neq p_1$.

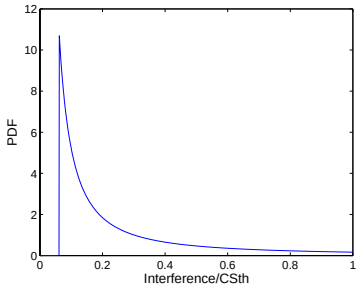

Figure 5: PDF of the interference given the existence of one interference node.

To derive the attempt probability p, we define the following terms:

- $p_2 = \Pr\{E_1|\text{node } i\text{'s carrier sense range is idle}\}$;
- $p_3 = \Pr\{\text{node } i\text{'s carrier sense range is idle}|E\}$.

Obviously,

$$p = p_1 \times p_2 \times p_3. \quad (19)$$

p_1 can still be expressed as $p_1 = 2/(E(CW)+1)$ in multi-hop wireless networks. In what follows, we derive p_2 and p_3.

3.5.1 *Derivation of* p_3

The probability p_3 can be straightforwardly derived, i.e.,

$$p_3 = \frac{(1-p)^{\lambda\pi {R_{cs}}^2}}{(1-p)^{\lambda\pi {R_i}^2}} = (1-p)^{\lambda\pi(R_{cs}^2 - R_i^2)}. \quad (20)$$

3.5.2 *Derivation of* p_2

By the definition of CS_{th} under the interference model, the probability p_2 is equivalent to Pr{ the aggregate interference contributed by transmissions outside the carrier sense range $\leq CS_{th}$ | node i's carrier sense range is idle }. It depends on the distribution of the interference nodes outside CS_{th}.

By **(A6)**, we consider only the accumulative interference contributed by six 1^{st} tier interference nodes. These nodes are located in the ring area that is centered at node i with inner radius R_{cs} and outer radius $2 \times R_{cs}$. Let I_{total} denote the total interference, I_j the interference received when there are j active interference nodes, and $\Pr(j)$ the probability that there exist j interference nodes, which can be calculated with p and the number of

Table 2: Pr(**Interference** $< CS_{th}$)**.**

# of nodes	P(I$< CS_{th}$)
2	0.918
3	0.762
4	0.560
5	0.357
6	0.192

hosts in the ring area. Then the CDF of I_{total} can be expressed as

$$\Pr(I_{total} \leq x) = \sum_{j=0}^{6} \Pr(j) \times \Pr(I_j \leq x). \quad (21)$$

We consider first $\Pr(I_1 \leq x)$. If the interference node is located on the inner (outer) circle of the ring, then it contributes an interference level of CS_{th} ($CS_{th} \cdot (1/2)^{\theta}$). Moreover, $I_1 = k \cdot CS_{th}$ ($(1/2)^{\theta} \leq k \leq 1$) if and only if the interference node is located inside the ring area. Thus we have

$$\Pr(I_1 \leq k \cdot CS_{th}) = \frac{(k^{-\frac{1}{\theta}} + 2)(2 - k^{-\frac{1}{\theta}})}{3}, \quad (22)$$

and the PDF of I_1 can be expressed as

$$f(I_1) = \frac{2}{3} \times k^{-\frac{\theta+2}{\theta}}. \quad (23)$$

Because $I_{j+1} = I_j + I_1$ ($1 \leq j \leq 5$), we can obtain the PDF of I_{j+1} by performing the convolution of the PDF of I_j and that of I_1. With the PDF of I_j ($1 \leq j \leq 6$), p_2 can be expressed as

$$p_2 = \Pr(I_{total} < CS_{th}), \quad (24)$$

where the CDF of I_{total} is given in Eq. (21).

3.6 Derivation of Collision Probability and Collision Period

In a WLAN, collisions are only caused by *simultaneous* transmissions within the WLAN. (Note that simultaneous transmission cannot be avoided even with the use of physical carrier sense.) However, in a multi-hop wireless network, collisions can also occur when the accumulative interference contributed by *simultaneous* transmissions outside the interference range and/or *concurrent* transmissions outside the carrier sense range. To facilitate derivation of parameters of interest, $E(N_c)$ and $E(T_c)$, we classify collisions into three categories:

Type-1 : Collision caused by simultaneous transmissions *within* the interference range.

Type-2 : Collision caused by interference contributed by simultaneous transmissions *outside* the interference range but *within* the carrier sense range.

Type-3 : Collision caused by interference contributed by *concurrent* transmissions *outside* carrier sense range.

Let $E(N_{c,1})$, $E(N_{c,2})$, and $E(N_{c,3})$ denote respectively the expected number of type-1, type-2, and type-3 collisions in a virtual transmission time, and $E(T_{c,1})$, $E(T_{c,2})$, and $E(T_{c,3})$ respectively the expected length of a type-1, type-2, and type-3 collision period in a virtual transmission time. In what follows, we derive these parameters.

3.6.1 Derivation of $E(N_{c,1}$ and $E(T_{c,1})$

Type-1 collisions are those considered in WLANs, and hence we can reuse the expressions given in Calí's model [4] directly

$$E(N_{c,1}) = \frac{1 - (1-p)^M - Mp(1-p)^{M-1}}{P(\textit{successful transmission})}, \quad (25)$$

and

$$E(T_{c,1}) = \frac{t_{slot}}{1 - (1-p)^M - Mp(1-p)^{M-1}} \times [\sum_{h=0}^{\infty} \{h \times [(1 - pq^h)^M - (1 - pq^{h-1})^M]\} - \frac{Mp(1-p)^{M-1}}{1-q}], \quad (26)$$

except that the term $P(\textit{successful transmission})$ (i.e., the probability of a successful transmission within an interference range) in Eq. (25) has to be re-derived. We will derive this expression below.

3.6.2 Derivation of $E(N_{c,2})$ and $E(T_{c,2})$

Note that although a single transmission outside the interference range of a receiver will not corrupt the on-going transmission, accumulative interference from multiple *simultaneous* transmissions may. Let $I_{(R_i,R_{cs})}$ denote the accumulative interference contributed by simultaneous transmissions outside R_i but within R_{cs}. It is easy to see that when $\frac{P/R_{tx}^{\theta}}{I_{(R_i,R_{cs})}} \leq \beta$, collision occurs. Let p_4 be defined as the probability that accumulative interference contributed by simultaneous transmissions outside R_i but within R_{cs} leads to collision. Then

$$p_4 = \Pr(I_{(R_i,R_{cs})} \geq \frac{P}{\beta \cdot R_{tx}^{\theta}}). \quad (27)$$

The derivation of p_4 is similar to that of $1 - p_2$ in Section 3.5, except that (i) the ring area is now with the inner radius R_i and the outer radius R_{cs}; and (ii) the number of simultaneously transmitting nodes could be more than 6, and hence the upper limit in the sum term of Eq. (21) can, in principle, go to infinity. (In our numerical examples, we set the upper limit to ℓ such that summing beyond ℓ does not further increase p_4.)

With the expression of p_4, $E(N_{c,2})$ and $E(T_{c,2})$ can now be expressed as

$$E(N_{c,2}) = \frac{p_4 \times Mp(1-p)^{M-1}}{P(\textit{successful transmission})}, \quad (28)$$

and

$$E(T_{c,2}) = \bar{m} = \frac{t_{slot}}{1-q}. \quad (29)$$

Note that $E(T_{c,2})$ is different from $E(T_{c,1})$. This is because $E(T_{c,1})$ is the same as $E[T_c]$ in a single-cell network, in which the collision period is the duration of the longest frame among multiple simultaneous transmissions that are involved in the collision. However, when a type-2 collision occurs, there is only one transmission within the interference range. Thus the collision period *from the perspective of nodes in this interference range* is one transmission duration (whose expected value is $\bar{m}$).

3.6.3 Derivation of $E(N_{c,3})$ and $E(T_{c,3})$

Consider an on-going transmission. If the transmission does not incur a collision due to simultaneous transmissions in the first slot, then in the course of transmission (the average duration of which is $\bar{m} = \frac{t_{slot}}{1-q}$), nodes within CS_{th} will keep silent, while the accumulative interference contributed by *concurrent* transmissions outside CS_{th} may still corrupt the transmission. By **(A6)**, we consider the accumulative interference, I_{total}, contributed by the six 1^{st}-tier interference nodes outside R_{cs}. Again, when $\frac{P/R_{tx}^{\theta}}{I_{total}} \leq \beta$, collision occurs. Thus the probability, p_5, that accumulative interference contributed by concurrent transmissions outside R_{cs} leads to collision can be expressed as

$$p_5 = \Pr(I_{total} \geq \frac{P}{\beta \cdot R_{tx}^{\theta}}). \quad (30)$$

Figure 6 illustrates how we calculate I_{total} as perceived by node N_0. The six 1_{st} tier interference nodes are located in the ring area centered at node N_0 and with inner (outer) radius of R_{cs} ($2R_{cs}$). The ring is divided into six sectors with equal proportion. In each sector there is one and only one interference node. Let I_i ($1 \leq i \leq 6$ denote the interference at the receiver D_0 contributed by the interference node in the ith sector. Then I_{total}=$\Sigma_{i=1}^{6} I_i$ denote the total interference. In practice, it is very difficult, if not impossible, to derive I_{total} because the six sectors are asymmetric irregular areas with respect to the receiver D_0. However, the interference, I_1, contributed by the interference node in the first sector dominates I_{total} since this interference node is closest to D_0. Hence, we approximate I_{total} by I_1, and only consider the shaded sector in Figure 6.

Let m denote the number of nodes in the shaded sector. Each of them transmits with a (likely different) attempt probability p. By Eq. (19), we need to derive p_1, p_2, and p_3. The probabilities p_1 and p_3 are the same for all nodes, while p_2 differs. This is because with respect to a node, say N_k, in the shaded sector, its 1^{st} tier interference node in the 4^{th} sector is fixed (i.e., N_0), and hence p_2 becomes the conditional probability that the total interference is less than CS_{th} given that N_0 transmits. Let $p_2^{(k)}$ denote p_2 with respect to node N_k in the shaded area, $I_0^{(k)}$ the interference contributed by N_0 and perceived at node N_k, and $I_{left}^{(k)}$ the remaining cumulative interference (perceived at node N_k) from the other five 1^{st}-tier interference nodes. Then $I_{left}^{(k)}$=I_{total}-$I_0^{(k)}$. Moreover we have

$$p_2^{(k)} = \Pr(I_{left}^{(k)} < (CS_{th} - I_0^{(k)})). \quad (31)$$

$I_{left}^{(k)}$ can be derived in the same manner as in Eq. (21), except that there are at most five 1^{st}-tier nodes and the entire ring area becomes $\frac{5}{6}$ of the ring. As shown in Eq. (31) if N_k is located at a position farther away from N_0, $p_2^{(k)}$ is larger. This implies that nodes which are more likely to induce collision at D_0 has a smaller attempt probability, thanks to the effect of physical carrier sense.

With I_{total} being approximated by I_1, p_5 is equal to the probability that the distance between the interference node, $N_{1,k}$ in the 1^{st} sector and D_0, denoted by $d_{N_{1,k},D_0}$, is smaller than the interference range R_i. Specifically, p_5 can be expressed as

$$p_5 = \Pr(d_{N_{1,k},D_0} \leq R_i) = \frac{\Sigma_{i=1}^{m} Ind(d_{N_{1,i},D_0} \leq R_i) \times p^{(i)}}{\Sigma_{i=1}^{m} p^{(i)}}$$
$$= \frac{\Sigma_{i=1}^{m} Ind(d_{N_{1,i},D_0} \leq R_i) \times p_2^{(i)}}{\Sigma_{i=1}^{m} p_2^{(i)}}$$

where $Ind(x)$ is an indicator function of x. When R_{cs} is smaller than $(1+\beta^{\frac{1}{\theta}}) \times R_{tx}$, p_5 is non-zero. Note that Eq. (32) is in descrete form and requires the knowledge of the number of nodes: m. When m is large we can use integral to calculate p_5.

With the expressions of p_4 (Eq. (27)) and p_5 (Eq. (32)), $E(N_{c,3})$ and $E(T_{c,3})$ can now be expressed as

$$E(N_{c,3}) = \frac{p_5 \times Mp(1-p)^{M-1} \times (1-p_4)}{P(\textit{successful transmission})}, \quad (32)$$

and

$$E(T_{c,3}) = \bar{m} = \frac{t_{slot}}{1-q}. \quad (33)$$

3.6.4 Derivation of P(successful transmission)

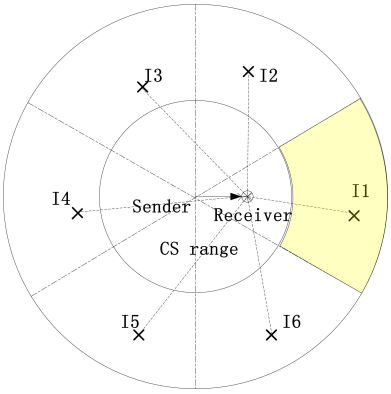

Figure 6: An example that illustrates how p_5 is calculated.

What is yet to be derived is $P(\textit{successful transmission})$ A successful transmission occurs if and only if the following three conditions hold: 1) in the first slot of transmission, no type-1 collision occurs; 2) in the first slot, no type-2 collision occurs; 3) in the 2^{nd} to n^{th} slots, no type-3 collision occurs. $P(\textit{successful transmission})$ is then expressed as

$$P(\textit{successful transmission}) = Mp(1-p)^{M-1}(1-p_4)(1-p_5). \quad (34)$$

By plugging Eqs. (15), (25) – (34) into Eq. (2), we obtain Eq. (35).

4. DISCUSSION

In this section, we discuss several insights that are shed from the analytical model, which can be used as the guideline for setting MAC parameters.

The first observation is that while the average contention window size is set to $\frac{2}{p} - 1$ in WLANs, it can be set to a smaller value in multi-hop networks. This is because as revealed in Eq. (19), the attempt probability not only is a function of the contention window size (through p_1), but also takes into account of physical carrier sense (through p_2 and p_3). In order to ensure the attempt probability remains large enough to improve the system throughput, the contention window size should be set to a larger value than that in WLANs.

The second observation is that while the optimal throughput can be achieved with the use of a larger value of p, it also leads to a larger collision probability. As a matter of fact, there exists a tradeoff between spatial reuse and collision caused by concurrent transmission. A larger value of p can increase the collision probability, but can also promote spatial reuse by by reducing the idle period in multi-hop networks. By comparing Eqs. (5) and (18), one can see that if the p value were set to the same value as that in WLANs, the idle period would be larger than its counterpart in WLANs. This is because an idle period may also occur in a "cell" when all the nodes in the cell are being silenced by sender nodes outside the cell but within their carrier sense ranges. This suggests that the p value should be set to a larger value in order to compensate this effect and promote spatial reuse.

5. SIMULATION RESULTS

In this section, we carry out a simulation study to validate the analytical model, to verify the observation made on the model, and to study the impact of the contention window size and the carrier sensing range on the system performance. As *ns-2* (we use ns-2.27 but what we discuss here is generally still true in the most recent release ns-2.29) does not take into account of the effect of accumulative interference, we first modify *ns-2* to incorporate that effect in order to improve the simulation fidelity.

5.1 Simulation setup

The scenario used in the simulation study is as follows. There are a total of 480 nodes, half of which are senders and the other half are receivers. The 240 senders are uniformly distributed in a 900m×900m square area, and each receiver is located 80 meters away from its sendere, with R_{tx}=80m. Every source sends its packets directly to its intended receiver. Note that our primary focus is on how the various MAC parameters impact the system throughput. In order to eliminate the coupling effect of routing and MAC, we deliberately position the receiver one-hop away from its sender. We run simulation under two data rates: 2Mbps (SINR threshold = 4db) and 6Mbps (SINR threshold = 6db). For each data rate, the contention window size varies from 8 to 256 and R_{cs} varies from 140 meters to 220 meters. Every sender sends CBR packets of size 512 KB.

5.2 Model validation

In section 3 we use p_2 and p_3 to characterize the effect of physical carrier sense on the attempt probability (p). The derivation of p_2 and p_3 is rigorous, except that we assume that the cumulative interference is mainly contributed by 1^{st} inteference nodes. However, when the contention window size becomes too small, p_2 and p_3 become smaller than they actually are in the simulation. As a result, p_2 and p_3 in the model exaggerate the effect of carrier sense and give a pessimistic value of p. To deal with this problem, we enforce the following rule: $p_2(p_3)$=ϕ if $p_2(p_3)$< ϕ, where ϕ ranges between 0.1 and 0.5 according to the ratio of R_{cs} and R_i. Fig. 7 gives both the theoretical and simulation results of the per-node throughput for the cases of bandwidth=2M and bandwidth=6M un-

$$t_v = \sum_{i=1}^{3} E\left(N_{c,i}\right) \cdot \left(E\left(T_{c,i}\right) + DIFS + SIFS + ACK\right) + \sum_{1}^{3} \left(E\left(N_{c,i}\right) + 1\right) \cdot E\left(I\right) + \bar{m} + SIFS + ACK + DIFS, \quad (35)$$

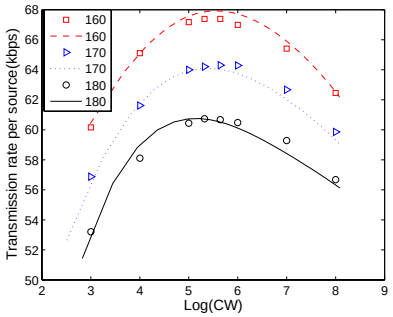

bandwidth = 2M

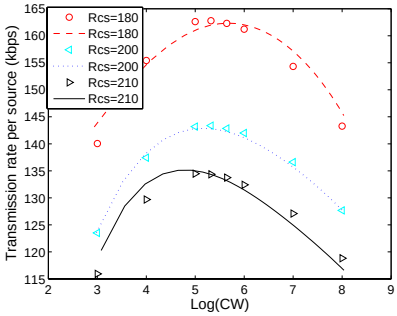

bandwidth=6M

Figure 7: The throughput attained by each node. Noe that continuous curves represent theoretical calculations, while discrete dots represent simulation results.

der three different values of R_{cs}. The two types of results agree quite well, especially in the vicinity of the optimal points. One interesting observation of Fig. 7 is that all the curves are quite flat in the range of CW$\in$[32,64]. Within this range, the difference in the per-node throughput is less than 1%. This is in sharp contrast to the results obtained in WLANs where the system throughput varies more dramatically [4]. This is perhaps because when the contention window size increases, the rate of change in p is smaller in multi-hop wireless networks Recall that p_2 and p_3 increases as the contention window size increases, and p is proportional to p_2 and p_3. As a result, when the contention window size increases, the rate at which p decreases is slower than in WLANs.

Another interesting observation is that the contention window size that achieves the optimal per-node throughput in multi-hop networks is much smaller than that in WLANs. Based on Calí's model, the optimal CW is 137 in the case of bandwidth = 2M and 107 in the case of bandwidth = 6M, respectively. In constrast, our simulation results show that in the six cases reported, the optimal contention window size is less than 64. There are two major reasons that may account for this observation. First, in multi-hop networks, R_{cs} is usually chosen to be larger than the interference range R_i in order to avoid the hidden terminal problems. With physical carrier sense, a pair of nodes within $R_{cs}(> R_i)$ of each other cannot transmit, unless they transmit simultaneously. A smaller contention window size (or equivalently a larger attempt probability) is thus desired to increase the probability of simultaneous transmission and promote spatial reuse. Second, recall

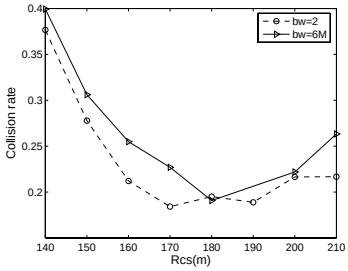

Figure 8: Collision ratio when the optimal per-node throughput is achieved

that p_2 and p_3 characterize the effect of physical carrier sense in the attempt probability p in multi-hop networks, while p_1 is related to the contention window size through $p_1 = 2/(E(CW) + 1)$. If the contention window size were set to the same value as that in WLANs, the $p(= p_1 \times p_2 \times p_3)$ would be smaller than its counterpart in WLANs. This suggests use of a larger CW value to obtain the optimal per-node throughput.

5.3 Analysis of the collision rate

Fig. 8 gives the simulation results of the collision ratio, i.e., the number of collisions divided by the total number of transmission attempts, when the optimal per-node throughput is achieved for a give value of R_{cs} by adjusting CW. The collision ratio is higher than 20% when the throughput is maximized. This implies that one cannot achieve high throughput and low packet loss at the same time. An interesting finding is that the collision ratio first increases and then decreases with the increase in R_{cs}. This supports our assertion that when R_{cs} is large, moderately increasing the CW

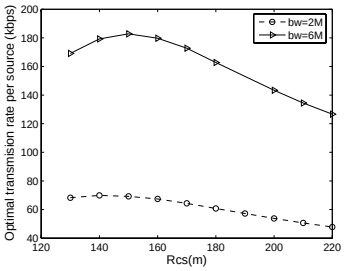

Figure 9: Optimal per-node throughput for given carrier sense range

size can improve the throughput although it also leads to the increase in collisions.

5.4 Optimal carrier sense range

Fig. 9 shows the optimal throughput versus R_{cs}. The optimal value of R_{cs} is 140m in the case of bandwidth=2M and 150m in the case of bandwidth=6M. Both are much smaller than those determined by $CS_{th,1}$ in the pessimistic model (Section 2) (by 50m and 55m, respectively). On the other hand, Fig. 10 gives the collision ratio when the optimal throughput is achieved. One important observation is that when R_{cs} is set to be smaller than that determined by $CS_{th,1}$ (i.e., 190m and 205m, repectively) the collision ratio also increases. When R_{cs} is large, we can always increase the contention window size in order to control the collision ratio within a certain bound. When R_{cs} is smaller than the carrier sense range determined by $CS_{th,1}$, the corresponding collision ratio is always above 20% and cannot be well controlled by adjusting the CW size.

6. CONCLUSION

In this paper, we propose a new analytical model that extends Calí's model to multi-hop wireless networks and incorporates the effects of physical carrier sense, SINR, and collision caused by accumulative interference. We carefully identify the parameters that are needed to re-defined and re-derived. The model is then validated through simulation. Our model can be used to determine the optimal contention window size and the carrier sensing range, as well as to give insights on explaining the behavior of multi-hop wireless networks. For example, it shows that in multi-hop networks, physical carrier sense and contention window size jointly determine the attempt probability of a node. It also points out that in multi-hop networks the optimal per-node throughput can be achieved using a smaller contention window at the expense of a higher collision ratio.

We have identified two future research issues. First, the analytical results deviate from the simulation results when the contention window size is too small. This is perhaps because the effect of physical carrier sense on reducing the attempt probability is aggravated in the derivation (i.e., $p = p_1 \times p_2 \times p_3$). We can alleviate this problem by characterizing more faithfully the dependence of media access among nodes that are close to each other. Second, because we focus on the impact of MAC parameters on the system throughput, we deliberately do not consider in this paper the coupling effect of routing and MAC and the intra-flow interference problem (that arises from the perspective of end-to-end throughput). After understanding better how to tune MAC parameters, we will incorporate into the model the effects of routing and intra-flow interference.

7. REFERENCES

[1] Ieee standard for wireless lan medium access control (mac) and physical layer (phy) specifications. ISO/IEC 802-11: 1999(E), Augest 1999.

[2] G. Bianchi. Performance analysis of the IEEE 802.11 distributed coordination function. *IEEE J. on Select. Areas in Commun.*, 18(3), 2000.

[3] Arvind Krishna Bruce Hajek and Richard O. LaMaire. On the capture probability for a larger number of stations. *IEEE Trans. on Commun.*, 45(2):254–260, 1997.

[4] F. Cali, M. Conti, and E. Gregori. Dynamic tuning of the ieee 802.11 protocol to achieve a theoretical throughput limit. *IEEE/ACM Trans. on Networking*, 8(6), December 2000.

[5] F. Cali, M. Conti, and E. Gregori. IEEE 802.11: design and performance evaluation of an adaptive backoff mechanism. *IEEE J. on Select. Areas in Commun.*, 18(9), September 2000.

[6] Matthias Grossglauser and David Tse. Mobility increases the capacity of ad-hoc wireless networks. In *Proc. of IEEE INFOCOM*, 2001.

[7] Kyle Jamieson, Bret Hull, Allen K. Miu, and Hari Balakrishnan. Understanding the real-world performance of carrier sense. In *ACM SIGCOMM Workshop on Experimental Approaches to Wireless Network Design and Analysis (E-WIND)*, Philadelphia, PA, August 2005.

[8] L. Lily Yang Jing Zhu, Xingang Guo and W. Steven Conner. Leveraging spatial reuse in 802.11 mesh networks with enhanced physical carrier sensing. In *IEEE International Conference on Communications*, June 2004.

[9] Hwangnam Kim, Jennifer C. Hou, Chunyu Hu, and Ye Ge. Qos provisioning for ieee 802.11-compliant wireless networks: past, present, and future. *Computer Networks Journal*, 2006. (to appear).

[10] A. Kumar, E. Altman, D. Miorandi, and M. Goyal. New insights from a fixed point analysis of single cell IEEE 802.11 WLANs. In *Proc. of IEEE INFOCOM*, April 2005.

[11] W. C. Y. Lee. Elements of cellular mobile radio systems. *IEEE Trans. on Vehicular Technology*, VT-35(2):48–56, May 1986.

[12] K. Medepalli and F.A. Tobagi. Towards

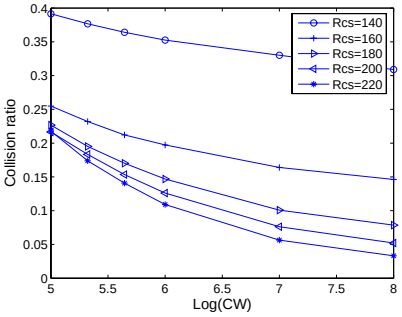

bw=2M

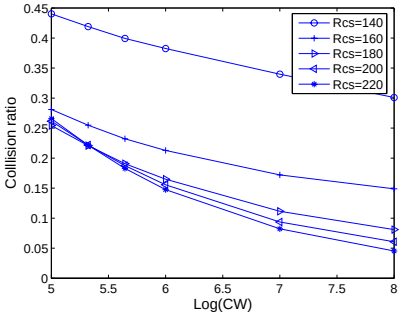

bw=6M

Figure 10: collision ratio (bw=2,6)

performance modeling of IEEE 802.11 based wireless networks: A unified framework and its applications. In *Proc. of IEEE INFOCOM*, April 2006.

[13] Xue Yang and Nitin H. Vaidya. On the physical carrier sense in wireless ad hoc networks. In *Proc. of IEEE INFOCOM*, 2005.

[14] H. Zhai and Y. Fang. Physical carrier sensing and spatial reuse in multirate and multihop wireless ad hoc networks. In *Proc. of IEEE INFOCOM*, 2006.